

SECOND-ORDER DIFFERENTIAL ADAPTIVE MICROPHONE ARRAY

Gary W. Elko, Jens Meyer

mh acoustics
25A Summit Ave
Summit, NJ 07901, USA

ABSTRACT

An adaptive second-order differential microphone design is proposed here that is constructed from a weighted sum of omnidirectional microphones. Theoretically, only three microphones are required to form a second-order array. The three microphone signals are combined to form three unique fixed second-order beams. Any second-order differential beam-pattern can be realized using a weighted sum of these three “building-block” beam outputs. If certain simple constraints are placed on the weighting of the three fixed beams, the two null locations that define the final second-order beampattern can be constrained to defined angular regions.

Index Terms— adaptive microphone beamforming

1. INTRODUCTION

The combination of small compact transducers and sophisticated digital signal processing now offer the possibility of improving the well-known problem of sound pick-up in noise. Reverberation can also seriously degrade microphone reception of speech signals. Over the past decades directional microphone arrays have proven to be effective in combating both of these problems.

This paper covers the design and implementation of an adaptive second-order differential microphone. The differential realizations presented here are extensions to the first-order implementation described in previous publications [1,2]. The adaptive self-optimization is based on minimizing the microphone output power under the constraints of a) the two independent nulls for second-order differential microphones are located in some defined angular region, typically the rear-half plane and b) sound from the look direction has a predefined frequency response, ideally a dirac impulse response. This constraint is realized by the weighted sum of time-delayed outputs from three closely-spaced omnidirectional microphones. Although the solution presented here does not always maximize the signal-to-noise ratio, it can significantly improve the signal-to-noise ratio in acoustic fields where only a few dominant noise sources are present.

2. DERIVATION OF THE ADAPTIVE SECOND-ORDER ARRAY

For a plane-wave signal $s(t)$ with spectrum $S(\omega)$ and wavevector \mathbf{k} incident on a three-element array with displacement vector d shown in Figure 1, the output can be written as,

$$Y_2(\omega, \theta) = S(\omega) (1 - e^{-j(\omega T_1 + \mathbf{k} \cdot \mathbf{d})}) (1 - e^{-j(\omega T_2 + \mathbf{k} \cdot \mathbf{d})}) = S(\omega) (1 - e^{-j\omega(T_1 + (d \cos \theta)/c)}) (1 - e^{-j\omega(T_2 + (d \cos \theta)/c)}) \quad (1)$$

where $d = |\mathbf{d}|$ is the element spacing for the first-order and second-order sections. The delay T_1 is equal to the delay applied to one sensor of the first-order sections and T_2 is the delay applied to the combination of the two first-order sections. Figure 1 shows a diagram of a second-order microphone composed of three omnidirectional microphones and three delays. The subscript on the variable Y is used to designate that the system response is a second-order differential response. The magnitude of the wavevector k is, $|k| = k = \omega/c$ and c is the speed of sound. Taking the magnitude of Eq. 1 and assuming $kd_1, kd_2 \ll \pi$ and, $\omega T_1, \omega T_2 \ll \pi$ yields,

$$|Y_2(\omega, \theta)| \approx \omega^2 |S(\omega) (T_1 + (d_1 \cos \theta)/c) (T_2 + (d_2 \cos \theta)/c)| \approx k^2 |S(\omega) [c^2 T_1 T_2 + c(T_1 d_2 + T_2 d_1) \cos \theta + d_1 d_2 \cos^2 \theta]| \quad (2)$$

The terms inside the brackets in Eq. 3 contain the array direc-

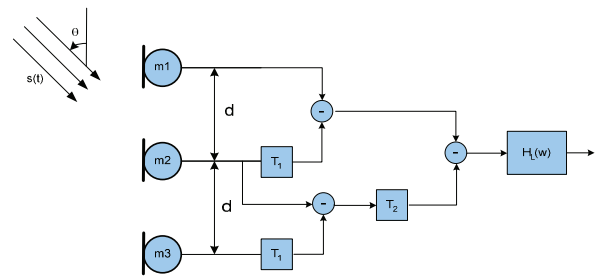


Fig. 1. Three-element microphone array used to form a second-order differential array

tional response, composed of a monopole term, a first-order

dipole term $\cos \theta$ that resolves the component of the acoustic particle velocity along the sensor axis, and a linear quadruple term $\cos^2 \theta$. One thing to notice in Eq. 3 is that the second-order array has a second-order differentiator frequency dependence (output increases quadratically with frequency). This frequency dependence is easily compensated in practice by a second-order lowpass filter.

An obvious realization of the second-order adaptive differential array with variable time delays T_1 and T_2 is shown in Figure 1. However, this solution is not attractive as it requires the ability of generating *any* time delay less than or equal to d_i/c . The computational requirements needed to realize the general delay by interpolation filtering and the resulting adaptive algorithms are unattractive for a real-time implementation. Fortunately there is a much simpler way to implement the adaptive differential array by using an extension of the back-to-back cardioid configuration described in an earlier paper [2].

Figure 2 shows a schematic implementation of an adaptive second-order array differential microphone utilizing only fixed delays and three omnidirectional microphone elements. The back-to-back cardioid arrangement for a second-order array can be implemented as shown in Figure 2. This topology can be followed to easily extend the differential array to any desired order. One simplification utilized here is the assumption that d_1 is equal to d_2 , although this is not necessary to realize the second-order differential array. This simplification does not limit the design but greatly simplifies the design and analysis. There are other benefits to the implementation that result by assuming that all d_i are equal: the major benefit being the need for only one unique delay element. For digital signal processing, this delay can be most simply realized as one sampling period, but since fractional delays are relatively easy to implement, this advantage is not really that significant. Furthermore, by setting the sampling period equal to d/c the back-to-back cardioid microphone outputs can be formed directly. Thus, if one chooses the spacing and the sampling rates appropriately, it is only necessary to store a few sequential sample values from each microphone signal to form the desired second-order directional response of the array. As previously discussed, the lowpass filter shown following the output $y(t)$ in Figure 2 is used to compensate the second-order ω^2 differentiator response.

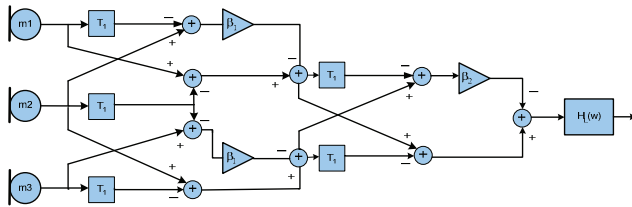


Fig. 2. Schematic implementation of an adaptive second-order differential array using only fixed delay elements.

3. IMPLEMENTATION OF A SECOND-ORDER ADAPTIVE ARRAY

Figure 3 shows a basic block diagram of the second-order adaptive array. Three microphone signals are fed into a fixed beamformer stage. This first stage forms three base beam-patterns, which are then fed to the adaptive beamformer. The three base patterns are the second-order forward cardioid (c_{ff}), the second-order backward cardioid (c_{bb}) and the second-order torus (c_{tt}). The adaptive beamformer operates on these base-beamformed signals to generate an overall output for the system.

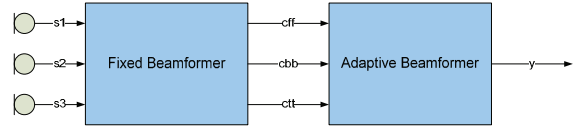


Fig. 3. Block diagram of second-order adaptive array

3.1. Fixed Beamformer

In Figure 3 one can see the details of the fixed beamformer which actually consists of three beamformers, one for each output beam. The fixed beamformers require a delay element that generates a delay of $T_1 = \tau = d/c$, where d is the microphone spacing and c is the speed of sound. Ideally the delay is matched to the sampling rate so that the delay time can be realized with an integer number of samples. Otherwise an interpolation filter is required. All delays in the fixed beamformers are identical. Note that the c_{tt} (toroid) output is amplified by a factor of two. This is done to simplify the adaptive beamformer notations.

It is instructive to compute the frequency and angular responses of these three second-order beam patterns. To begin, let us assume that the microphones measure the acoustic pressure with a flat frequency response so the microphone signals s_1, s_2, s_3 are within a scale factor, the acoustic pressures p_1, p_2, p_3 . With this assumption, and the assumptions that the time delays $T_1 = \tau$ are equal to d/c (the time it takes sound to propagate between each pair of microphones for on-axis incidence) and the spacing d is much less than the acoustic wavelength, the three normalized second-order beam outputs can be written for the forward second-order cardioid as,

$$c_{ff} = \frac{1}{4}[p_1 - 2p_2e^{-j\omega\tau} + p_3e^{-2j\omega\tau}] \approx \frac{1}{4}[-e^{-j\omega\tau}(\omega\tau)^2(1 + \cos \theta)^2] \quad (3)$$

and for the second-order backwards cardioid,

$$c_{bb} = \frac{1}{4}[p_1e^{-2j\omega\tau} - 2p_2e^{-j\omega\tau} + p_3] \approx \frac{1}{4}[-e^{-j\omega\tau}(\omega\tau)^2(1 - \cos \theta)^2] \quad (4)$$

and finally for the second-order toroid,

$$\begin{aligned} c_{tt} &= -p_1 e^{-j\omega\tau} + p_2(1 + e^{-2j\omega\tau}) - p_3 e^{-j\omega\tau} \\ &\approx -e^{-j\omega\tau} (\omega\tau)^2 \sin^2 \theta \end{aligned} \quad (5)$$

As can be seen in the above equations, each of the second-order outputs exhibits the second-order high-pass frequency response. This second-order high-pass response has implications to the output signal-to-noise ratio as will be shown in more detail in a later section. It can also be seen that all the patterns are phase centered relative to the center of the array and all of the same phase since the nulls of each pattern are second-order nulls and therefore there are no phase reversals in the beampattern. This property of not having phase reversals in the beampattern is important in the overall design and operation of the adaptive beamformer. It can also be seen that there is a delay in the output of the arrays equal to the time delay used in the beamformer.

3.2. Adaptive beamformer

An overview of the adaptive beamformer is plotted in Figure 4. The adaptive beamformer receives the three base-beamformed signals and applies a standard normalized LMS algorithm with the following update equation:

$$\alpha_{t+1} = \alpha_t + \frac{\mu c e}{c^T c + \delta} \quad (6)$$

In Equation 6 α is the coefficient vector,

$$\alpha = [\alpha_1(t) \ \alpha_2(t)]^T \quad (7)$$

c is the signal vector

$$c = [c_{bb}(t) \ c_{tt}(t)]^T \quad (8)$$

and the error signal e is computed according to

$$e = c_{ff} - \alpha^T c. \quad (9)$$

Note that the error signal also serves as the output of the adaptive beamformer. δ represents a regularization constant that is used to control the adaptation update when the denominator gets small and μ is the step-size.

Note that the adaptive beamformer does not require any constraints for the look-direction response. This is inherently included in the forward-cardioid base pattern. In order to limit the position of the zeros, a constraint on α is necessary. A simple but effective constraint is $-1 \leq \alpha_{1,2} \leq 1$. This limits the zero in the beam-pattern to be out of the frontal angular region from 0 to 66 degrees.

The frequency response for the look-direction is determined by the on-axis response of the second-order forward cardioid which is

$$H(kd) = 2(1 - \cos(2kd)) = 4 \sin(kd)^2. \quad (10)$$

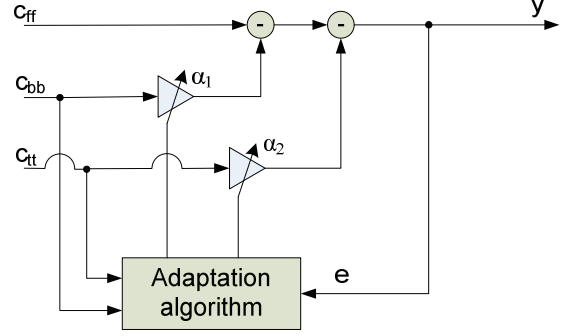


Fig. 4. Block diagram of the second-order adaptive beamformer

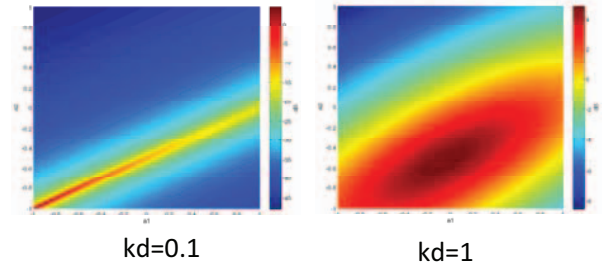


Fig. 5. WNG for second-order adaptive array for $kd=0.1$ (left, is equivalent to about 100 Hz for $d=60$ mm) and $kd=1$ (right, is equivalent to about 1 kHz for $d=60$ mm). Note the different scales for the plots (-48 to 4.8dB on the left and -8.5 to 4.8dB on the right).

In order to achieve a flat frequency response one has to compensate for this response. In the small kd region this can be done with a simple second-order lowpass filter. If the frequency range of the system goes beyond $kd < 1$ it might become necessary to implement a higher order approximation of Equation 10.

4. WHITE NOISE GAIN (WNG) CHARACTERISTIC

The WNG characteristic or its inverse, the noise sensitivity [3] describes the noise performance and also the robustness of the microphone array to perturbations from ideal values. For a fixed beamformer, the WNG is a function of frequency. Since we are dealing with an adaptive array with two degrees of freedom the WNG thus becomes a function in three variables. In order to visualize this result, the WNG for two frequencies ($kd=0.1$ and $kd=1$) is plotted as a surface plot in Figure 5 covering the allowed range of $\alpha_{1,2}$ (Equation 6).

The maximum WNG that can be achieved with 3 microphones is $10 \log_{10}(3) = 4.8$ dB. This is the maximum limit for both plots in Figure 5. For small kd the maximum WNG is achieved for $\alpha=[-1, -1]$ which is the omnidirectional pattern.

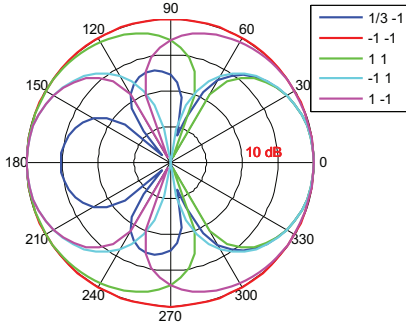


Fig. 6. Second-order beampatterns for a few values of α .

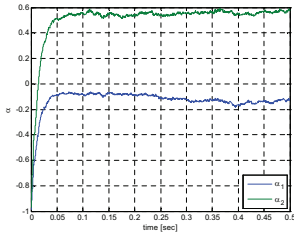


Fig. 7. Adaptive null angles for equal power sources at 0, 90, 150 degrees.

For $kd=1$ the small kd approximation is no longer valid and the in-phase addition of the 3 microphone signals is achieved for weighting different from $[-1, -1]$.

The smallest WNG varies significantly depending on kd . This can be explained by noting that as long as the low kd approximation is valid the sensor weightings do not change and the denominator for the WNG remains constant. On the other hand, the numerator follows Equation 10. Therefore with every doubling of kd the lower bound of the WNG will increase by 12 dB (or 40dB per decade). This is roughly true for the results shown in Figure 5. This effect reduces the dynamic range of the figure and the maximum becomes broader.

5. SIMULATIONS

The LMS algorithm has been implemented as a Matlab simulation. The simulation is performed at a sampling rate of 20 kHz with a microphone spacing of 1.7 cm (this simplified the implementation since the delay to form the forward/backward cardioids equals 1 sample). For the following examples the step-size is set to 0.01. Equal power white noise signals are generated from different angles. Figure 6 shows some predicted beampatterns for a few different values of α . Results for the case of two interfering noise sources at 90 and 150 degrees are shown in Figures 7 and 8.

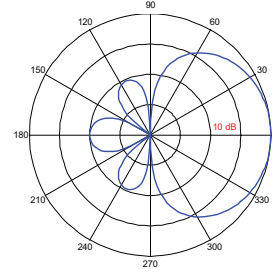


Fig. 8. Converged adaptive beampattern for equal power sources at 0, 90, 150 degrees.

6. CONCLUSIONS

A second-order adaptive differential microphone with two null angles constrained to a prescribed angular region has been presented. A simple NMLS adaptation algorithm was presented. Computer simulations showed that the null locations can be adapted within a very short period of time.

One direction that may be beneficial is to implement the adaptive array in frequency subbands. By allowing the nulls to move independently with frequency the adaptive array could hypothetically cancel out multiple noise sources that do not have frequency overlap. Also, in a multipath environment it is possible to exploit the spatial filtering of the adaptive array to reduce the diffuse reverberant field component up to 9.5 dB. Finally, if it is desirable to steer the beam to any direction in a plane, this can be done by building a 2D circular array [4]. Steering in all directions can be accomplished by using a spherical array geometry [5].

7. REFERENCES

1. G. W. Elko, "Differential Microphone Arrays", Chapter 2, *Audio Signal Processing for Next-Generation Multimedia Communication Systems*, Y. Huang, J. Benesty Eds, Kluwer Academic Publishers, 2004.
2. G.W. Elko, A.N. Pong, "A simple adaptive first-order differential microphone", Proceedings of the 1995 IEEE Workshop on Applications of Signal Processing to Audio and Acoustics, 1995, pp. 169-172.
3. E. N. Gilbert, S. P. Morgan, "Optimum design of directive antenna arrays subject to random variations". *Bell Syst. Tech. J.*, Vol. 34, pp 637-663, May 1955.
4. G. W. Elko, J. Meyer, "Spherical harmonic modal beamforming for an augmented circular microphone array". Proceedings ICASSP 2008.
5. J. Meyer, G. W. Elko, "A highly scalable spherical microphone array based on an orthonormal decomposition of the soundfield", Proceedings ICASSP 2002.